

# Stochastic Background of Relic Scalar Gravitational Waves tuned by Extended Gravity

Mariafelicia De Laurentis<sup>a</sup>, Salvatore Capozziello<sup>a</sup>

<sup>a</sup>Dipartimento di Scienze Fisiche, Università di Napoli “ Federico II”, INFN Sez. di Napoli, Compl. Univ. di Monte S. Angelo, Edificio G, Via Cinthia, I-80126, Napoli, Italy

A stochastic background of relic gravitational waves is achieved by the so called adiabatically-amplified zero-point fluctuations process derived from early inflation. It provides a distinctive spectrum of relic gravitational waves. In the framework of scalar-tensor gravity, we discuss the scalar modes of gravitational waves and the primordial production of this scalar component which is generated beside tensorial one. Then we analyze different viable  $f(R)$ -gravities towards the Solar System tests and stochastic gravitational waves background. The aim is to achieve experimental bounds for the theory at local and cosmological scales in order to select models capable of addressing the accelerating cosmological expansion without cosmological constant but evading the weak field constraints. It is demonstrated that viable  $f(R)$ -gravities under consideration not only satisfy the local tests, but additionally, pass the PPN-and stochastic gravitational waves bounds for large classes of parameters.

## 1. Introduction

The idea that General Relativity (GR) should be extended or corrected at large scales (infrared limit) or at high energies (ultraviolet limit) is suggested by several theoretical and observational issues [1]. Quantum field theory in curved spacetimes, as well as the low-energy limit of String/M theory, both imply semi-classical effective actions containing higher-order curvature invariants or scalar-tensor terms. In addition, GR has been definitely tested only at Solar System scales while it may show several shortcomings if checked at higher energies or larger scales. Besides, the Solar System experiments are, up to now, not conclusive to state that the only viable theory of gravity is GR: for example, the limits on PPN parameters should be greatly improved to fully remove degeneracies. Of course, modifying the gravitational action asks for several fundamental challenges. These models can exhibit instabilities or ghost-like behavior, while, on the other hand, they have to be matched with observations and experiments in the appropriate low energy limit. There exist cosmological solutions that give the accelerated expansion of the universe at late times. In addition, it has been discovered that some stability

conditions can lead to avoid ghost and tachyon solutions. Furthermore there exist viable  $f(R)$  models which satisfy both background cosmological constraints and stability conditions and results have been achieved in order to place constraints on  $f(R)$  cosmological models by CMBR anisotropies and galaxy power spectrum. Moreover, some of such viable models lead to the unification of early-time inflation with late-time acceleration. On the other hand, by considering  $f(R)$ -gravity in the low energy limit, it is possible to obtain corrected gravitational potentials capable of explaining the flat rotation curves of spiral galaxies or the dynamics of galaxy clusters without considering huge amounts of dark matter. Furthermore, several authors have dealt with the weak field limit of fourth order gravity, in particular considering the PPN limit and the spherically symmetric solutions. This great deal of work needs an essential issue to be pursued: we need to compare experiments and probes at local scales (e.g. Solar System) with experiments and probes at large scales (Galaxy, extragalactic scales, cosmology) in order to achieve self-consistent  $f(R)$  models. In order to constrain further viable  $f(R)$ -models, one could take into account also the stochastic background of gravi-

tational waves (GW) which, together with cosmic microwave background radiation (CMBR), would carry a huge amount of information on the early stages of the Universe evolution. In fact, if detected, such a background could constitute a further probe for these theories at very high red-shift [9]. On the other hand, a key role for the production and the detection of the relic gravitational radiation background is played by the adopted theory of gravity. This means that the effective theory of gravity should be probed at zero, intermediate and high redshifts to be consistent at all scales and not simply extrapolated up to the last scattering surface, as in the case of GR.

The aim of this report is to discuss the PPN Solar-System constraints and the GW stochastic background considering some recently proposed  $f(R)$  gravity models [2,3] which satisfy both cosmological and stability conditions mentioned above. Using the definition of PPN-parameters  $\gamma$  and  $\beta$  in terms of  $f(R)$ -models and the definition of scalar GWs [4], we compare and discuss if it is possible to search for parameter ranges of  $f(R)$ -models working at Solar System and GW stochastic background scale [5].

## 2. Extended Gravity

A action for scalar-tensor gravity in a Brans-Dicke-like form which can be adopted also for  $f(R)$ -gravity once a suitable scalar field is defined, is [6]

$$S = \int d^4x \sqrt{-g} \left[ \varphi R - \frac{\omega(\varphi)}{\varphi} g^{\mu\nu} \varphi_{;\mu} \varphi_{;\nu} - W(\varphi) + \mathcal{L}_m \right] \quad (1)$$

By varying the action (1) with respect to  $g_{\mu\nu}$ , we obtain the field equations

$$G_{\mu\nu} = -\frac{4\pi\tilde{G}}{\varphi} T_{\mu\nu}^{(m)} + \frac{\omega(\varphi)}{\varphi^2} (\varphi_{;\mu} \varphi_{;\nu} - \frac{1}{2} g_{\mu\nu} g^{\alpha\beta} \varphi_{;\alpha} \varphi_{;\beta}) + \frac{1}{\varphi} (\varphi_{;\mu\nu} - g_{\mu\nu} \square\varphi) + \frac{1}{2\varphi} g_{\mu\nu} W(\varphi) \quad (2)$$

while the variation with respect to  $\varphi$  gives the Klein - Gordon equation

$$\square\varphi = \frac{1}{2\omega(\varphi) + 3} [-4\pi\tilde{G}T^{(m)} + 2W(\varphi) + \varphi W'(\varphi) + \frac{d\omega(\varphi)}{d\varphi} g^{\mu\nu} \varphi_{;\mu} \varphi_{;\nu}]. \quad (3)$$

We are assuming physical units  $G = 1$ ,  $c = 1$  and  $\hbar = 1$ .  $T_{\mu\nu}^{(m)}$  is the matter stress-energy tensor and  $\tilde{G}$  is a dimensional, strictly positive, gravitational coupling constant [4,7]. The Newton constant is replaced by the effective coupling

$$G_{eff} = -\frac{1}{2\varphi}, \quad (4)$$

which is, in general, different from  $G$ . GR is recovered for

$$\varphi = \varphi_0 = -\frac{1}{2}. \quad (5)$$

## 3. Gravitational waves from Extended Gravity

In order to study gravitational waves, we assume first-order, small perturbations in vacuum ( $T_{\mu\nu}^{(m)} = 0$ ). This means

$$g_{\mu\nu} = \eta_{\mu\nu} + h_{\mu\nu}, \quad \varphi = \varphi_0 + \delta\varphi \quad (6)$$

and

$$W \simeq \frac{1}{2} \alpha \delta\varphi^2 \Rightarrow W' \simeq \alpha \delta\varphi \quad (7)$$

for the self-interacting, scalar-field potential. These assumptions allow to derive the "linearized" curvature invariants  $\tilde{R}_{\mu\nu\rho\sigma}$ ,  $\tilde{R}_{\mu\nu}$  and  $\tilde{R}$  which correspond to  $R_{\mu\nu\rho\sigma}$ ,  $R_{\mu\nu}$  and  $R$ , and then the linearized field equations [4,8]

$$\tilde{R}_{\mu\nu} - \frac{\tilde{R}}{2} \eta_{\mu\nu} = -\partial_\mu \partial_\nu \Phi + \eta_{\mu\nu} \square\Phi \quad (8)$$

$$\square\Phi = m^2 \Phi,$$

where

$$\Phi \equiv -\frac{\delta\varphi}{\varphi_0}, \quad m^2 \equiv \frac{\alpha\varphi_0}{2\omega + 3}. \quad (9)$$

In particular, the transverse-traceless (TT) gauge (see [8]) can be generalized to scalar-tensor gravity obtaining the total perturbation of a GW incoming in the  $z+$  direction in this gauge as

$$h_{\mu\nu}(t-z) = A^+(t-z)e_{\mu\nu}^{(+)} + A^\times(t-z)e_{\mu\nu}^{(\times)} + \Phi(t-z)e_{\mu\nu}^{(s)}. \quad (10)$$

The term  $A^+(t-z)e_{\mu\nu}^{(+)} + A^\times(t-z)e_{\mu\nu}^{(\times)}$  describes the two standard (i.e. tensorial) polarizations of a gravitational wave arising from GR in the TT gauge [8], while the term  $\Phi(t-z)e_{\mu\nu}^{(s)}$  is the extension of the TT gauge to the scalar case. This means that, in scalar-tensor gravity, the scalar field generates a third component for the tensor polarization of GWs. This is because three different degrees of freedom are present of [4,10], while only two are present in standard General Relativity.

#### 4. Stochastic background of relic scalar GWs

Then, for a purely scalar gravitational wave, the metric perturbation is [4,10,9]

$$h_{\mu\nu} = \Phi e_{\mu\nu}^{(s)}. \quad (11)$$

The stochastic background of scalar gravitational waves can be described in terms of the scalar field  $\Phi$  and characterized by a dimensionless spectrum (see the analogous definition for tensor modes in [4])

$$\Omega_{sgw}(f) = \frac{1}{\rho_c} \frac{d\rho_{sgw}}{d \ln f}, \quad (12)$$

where

$$\rho_c \equiv \frac{3H_0^2}{8\pi G} \quad (13)$$

is the (present) critical energy density of the universe,  $H_0$  is the Hubble parameter today, and  $d\rho_{sgw}$  is the energy density of the scalar gravitational radiation in the frequency interval  $(f, f+df)$ . We are now using standard units. Now it is possible to write an expression for the energy density of the stochastic scalar relic gravitons background in the angular frequency interval

$(\omega, \omega + d\omega)$  as

$$d\rho_{sgw} = 2\hbar\omega \left( \frac{\omega^2 d\omega}{2\pi^2 c^3} \right) N_\omega = \frac{\hbar H_{dS}^2 H_0^2}{4\pi^2 c^3} \frac{d\omega}{\omega} = \frac{\hbar H_{dS}^2 H_0^2}{4\pi^2 c^3} \frac{df}{f}, \quad (14)$$

where  $f$ , as above, is the frequency in standard comoving time. Eq. (14) can be rewritten in terms of the critical and de Sitter energy densities

$$H_0^2 = \frac{8\pi G \rho_c}{3c^2}, \quad H_{dS} = \frac{8\pi G \rho_{dS}}{3c^2}. \quad (15)$$

Introducing the Planck density  $\rho_{Planck} = \frac{c^5}{\hbar G^2}$ , the spectrum is given by

$$\Omega_{sgw}(f) = \frac{1}{\rho_c} \frac{d\rho_{sgw}}{d \ln f} = \frac{f}{\rho_c} \frac{d\rho_{sgw}}{df} = \frac{16}{9} \frac{\rho_{dS}}{\rho_{Planck}}. \quad (16)$$

At this point, some comments are in order. First, the calculation works for a simplified model that does not include the matter-dominated era. If the latter is included, the redshift at the equivalence epoch has to be considered. Taking into account Ref. [4,10] one gets

$$\Omega_{sgw}(f) = \frac{16}{9} \frac{\rho_{dS}}{\rho_{Planck}} (1+z_{eq})^{-1} \quad (17)$$

for the waves which, at the epoch in which the universe becomes matter-dominated, have a frequency higher than  $H_{eq}$ , the Hubble parameter at equivalence. This situation corresponds to frequencies  $f > (1+z_{eq})^{1/2} H_0$  today. The redshift correction in eq. (17) is needed since the present value of the Hubble parameter  $H_0$  would be different without a matter-dominated contribution. At lower frequencies, the spectrum is given by

$$\Omega_{sgw}(f) \propto f^{-2}. \quad (18)$$

Nevertheless, since the spectrum falls off as  $f^{-2}$  at low frequencies, today at *LIGO/VIRGO* and *LISA* frequencies, one gets

$$\Omega_{sgw}(f) h_{100}^2 < 2.3 \times 10^{-12}, \quad (19)$$

where  $h_{100} = H_0 / (100 \text{ km} \cdot \text{s}^{-1} \cdot \text{Mpc}^{-1})$ . It is interesting to calculate the corresponding strain

at  $f \sim 100\text{Hz}$ , where interferometers such as *VIRGO* and *LIGO* achieve maximum sensitivity. The well known equation for the characteristic amplitude adapted to the scalar component of gravitational waves

$$\Phi_c(f) \simeq 1.26 \times 10^{-18} \left( \frac{1 \text{ Hz}}{f} \right) \sqrt{h_{100}^2 \Omega_{sgw}(f)}, \quad (20)$$

can be used to obtain

$$\Phi_c(100 \text{ Hz}) < 2 \cdot 10^{-26}. \quad (21)$$

Then, since we expect a sensitivity of the order of  $10^{-22}$  for the above interferometers at  $f \sim 100 \text{ Hz}$ , we need to gain four orders of magnitude. Let us analyze the situation also at lower frequencies. The sensitivity of the *VIRGO* interferometer is of the order of  $10^{-21}$  at  $f \sim 10 \text{ Hz}$  and in that case it is

$$\Phi_c(10 \text{ Hz}) < 2 \cdot 10^{-25}. \quad (22)$$

The sensitivity of the *LISA* interferometer will be of the order of  $10^{-22}$  at  $f \sim 10^{-3} \text{ Hz}$  and in this case it is

$$\Phi_c(10^{-3} \text{ Hz}) < 2 \cdot 10^{-21}. \quad (23)$$

This means that a stochastic background of relic scalar gravitational waves could, in principle, be detected by the *LISA* interferometer [11].

### 5. $f(R)$ -gravity constrained by PPN parameters and stochastic background of GWs

A Brans-Dike-like theory with  $\omega = 0$  is dynamically equivalent to an  $f(R)$ -gravity, so the bounds coming from the interferometric ground-based (*VIRGO*, *LIGO*) and space (*LISA*) experiments could constitute a further probe for gravity if matched with bounds at other scales to achieve experimental bounds for the theory at local and cosmological scales. For our aims consider a class of  $f(R)$  models which do not contain cosmological constant and are explicitly designed to satisfy cosmological and Solar-System constraints in given limits of the parameter space. In practice, we

choose a class of functional forms of  $f(R)$  capable of matching, in principle, observational data. Firstly, the cosmological model should reproduce the CMBR constraints in the high-redshift regime (which agree with the presence of an effective cosmological constant). Secondly, it should give rise to an accelerated expansion, at low redshift, according to the  $\Lambda\text{CDM}$  model. Thirdly, there should be sufficient degrees of freedom in the parameterization to encompass low redshift phenomena (e.g. the large scale structure) according to the observations. Finally, small deviations from GR should be consistent with Solar System tests. All these requirements suggest that we can assume the limits

$$\lim_{R \rightarrow \infty} f(R) = \text{constant}, \quad (24)$$

$$\lim_{R \rightarrow 0} f(R) = 0, \quad (25)$$

which are satisfied by a general class of broken power law models, proposed in [3], which are

$$f_{HS}(R) = R - \lambda R_c \frac{\left(\frac{R}{R_c}\right)^{2n}}{\left(\frac{R}{R_c}\right)^{2n} + 1} \quad (26)$$

where  $m$  is a mass scale and  $c_{1,2}$  are dimensionless parameters. Besides, another viable class of models was proposed in [2]

$$f_S(R) = R + \lambda R_c \left[ \left(1 + \frac{R^2}{R_c^2}\right)^{-p} - 1 \right]. \quad (27)$$

Since  $f(R=0) = 0$ , the cosmological constant has to disappear in a flat spacetime. The parameters  $\{n, p, \lambda, R_c\}$  are constants which should be determined by experimental bounds. In Fig.(1), we have plotted the selected models as function of  $\frac{R}{R_c}$  for suitable values of  $\{p, n, \lambda\}$ .

The above models can be constrained at Solar System level by considering the PPN formalism. This approach is extremely important in order to test gravitational theories and to compare them with GR. One can derive the PPN-parameters  $\gamma$

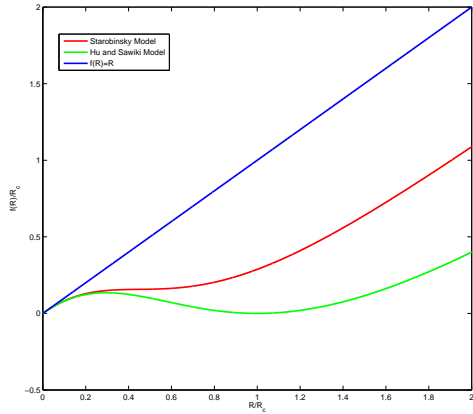


Figure 1. Plots of  $f(R)$  models as function of  $\frac{R}{R_c}$ . Model  $f_{HS}$  in Eq. (26) with  $n = 1$  and  $\lambda = 2$  (green line). Model  $f_S$  in Eq.(27) with  $p = 2$ ,  $\lambda = 0.95$  (red line). We also plot  $f(R) = R$  (blue line) to see whether or not the stability condition  $f_{,R} > 0$  is violated.

and  $\beta$  in terms of a generic analytic function  $f(R)$  and its derivative

$$\gamma - 1 = -\frac{f''(R)^2}{f'(R) + 2f''(R)^2}, \quad (28)$$

$$\beta - 1 = \frac{1}{4} \left[ \frac{f'(R) \cdot f''(R)}{2f'(R) + 3f''(R)^2} \right] \frac{d\gamma}{dR}. \quad (29)$$

These quantities have to fulfill the constraints coming from the Solar System experimental tests. They are the perihelion shift of Mercury, the Lunar Laser Ranging, the upper limits coming from the Very Long Baseline Interferometry (VLBI) and the results obtained from the Cassini spacecraft mission in the delay of the radio waves transmission near the Solar conjunction.

- Mercury perihelion Shift  $|2\gamma - \beta - 1| < 3 \times 10^{-3}$
- Lunar Laser Ranging  $4\beta - \gamma - 3 = (0.7 \pm 1) \times 10^{-3}$

- Very Long Baseline Interferometer  $|\gamma - 1| < 4 \times 10^{-4}$

- Cassini Spacecraft  $\gamma - 1 = (2.1 \pm 2.3) \times 10^{-5}$

Take into account the above  $f(R)$ -models, specifically, we have investigated the values or the ranges of parameters in which they match the above Solar-System experimental constraints. In other words, we use these models to search under what circumstances it is possible to significantly address cosmological observations by  $f(R)$ -gravity and, simultaneously, evade the local tests of gravity [5]. At this point, using the above LIGO, VIRGO and LISA upper bounds, calculated for the characteristic amplitude of GW scalar component, let us test the  $f(R)$ -gravity models. Taking into account the discussion in Sec. 2, we have that the GW scalar component is derived considering

$$\Phi = -\frac{\delta\sigma}{\sigma_0}, \quad \sigma = -\ln(1 + f'(R)) = \ln f'(A),$$

$$\delta\sigma = \frac{f''(A)}{1 + f'(A)} \delta A. \quad (30)$$

Finally we obtain a good sets of parameters for the Starobinsky model PPN vs GW-stochastic:

- $\frac{R}{R_c} = 3.38$ ,  $p = 1$ ,  $\lambda = 2$
- $\frac{R}{R_c} = \sqrt{3}$ ,  $p = 2$ ,  $0.944 < \lambda < 0.966$

and for Hu and Sawicki model

- $\frac{R}{R_c} = \sqrt{3}$ ,  $n = 2$ ,  $\lambda > \frac{8}{3\sqrt{3}}$

such sets of parameters are not in conflict with bounds coming from the cosmological stochastic background of GWs and, some sets reproduce quite well both the PPN upper limits and the constraints on the scalar component amplitude of GWs. The results indicate that self-consistent models could be achieved comparing experimental data at very different scales without extrapolating results obtained only at a given scale [5].

## 6. Conclusions

We have investigated the possibility that some viable  $f(R)$  models could be constrained considering both Solar System experiments and upper

bounds on the stochastic background of gravitational radiation. Such bounds come from interferometric ground-based (VIRGO and LIGO) and space (LISA) experiments. The underlying philosophy is to show that the  $f(R)$  approach, in order to describe consistently the observed universe, should be tested at very different scales, that is at very different redshifts. In other words, such a proposal could partially contribute to remove the unpleasant degeneracy affecting the wide class of dark energy models, today on the ground.

Beside the request to evade the Solar System tests, new methods have been recently proposed to investigate the evolution and the power spectrum of cosmological perturbations in  $f(R)$  models. The investigation of stochastic background, in particular of the scalar component of GWs coming from the  $f(R)$  additional degrees of freedom, could acquire, if revealed by the running and forthcoming experiments, a fundamental importance to discriminate among the various gravity theories [9]. These data (today only upper bounds coming from simulations) if combined with Solar System tests, CMBR anisotropies, LSS, etc. could greatly help to achieve a self-consistent cosmology bypassing the shortcomings of  $\Lambda$ CDM model.

Specifically, we have taken into account two broken power law  $f(R)$  models fulfilling the main cosmological requirements which are to match the today observed accelerated expansion and the correct behavior in early epochs. We have taken into account the results of the main Solar System current experiments. Such results give upper limits on the PPN parameters which any self-consistent theory of gravity should satisfy at local scales. Starting from these, we have selected the  $f(R)$  parameters fulfilling the tests. As a general remark, all the functional forms chosen for  $f(R)$  present sets of parameters capable of matching the two main PPN quantities, that is  $\gamma_{exp}$  and  $\beta_{exp}$ . This means that, in principle, extensions of GR are not *a priori* excluded as reasonable candidates for gravity theories. To construct such extensions, the reconstruction method developed in may be applied.

The interesting feature, and the main result of this paper, is that such sets of parameters are not

in conflict with bounds coming from the cosmological stochastic background of GWs. In particular, some sets of parameters reproduce quite well both the PPN upper limits and the constraints on the scalar component amplitude of GWs [5,11].

Far to be definitive, these preliminary results indicate that self-consistent models could be achieved comparing experimental data at very different scales without extrapolating results obtained only at a given scale.

## REFERENCES

1. S. Capozziello and M. Francaviglia, *Gen.Rel.Grav.* **40**, pp 357-420, (2008).
2. A. A. Starobinsky, *JETP Lett.* **86**, 157 (2007).
3. W. Hu and I. Sawicki, *Phys. Rev. D* **76** 064004 (2007).
4. S.Capozziello, C.Corda, M. De Laurentis, *Mod. Phys. Lett. A*, vol. **22**, 2647,(2007).
5. S. Capozziello, M. De Laurentis, S. Nojiri, S.D. Odintsov, e-Print: arXiv:0808.1335 [hep-th].
6. C. Brans and R. H. Dicke, *Phys. Rev.* **124**, 925 (1961).
7. S. Capozziello, *Quantum Gravity Research Trends* Ed. A. Reimer, pp. 227-276 Nova Science Publishers Inc., NY (2005).
8. C. W. Misner , K. S. Thorne and J. A. Wheeler, "Gravitation" - W. H. Feeman and Company 1973.
9. S.Capozziello, C.Corda, M. De Laurentis *Mod. Phys. Lett. A* vol. **22** ,1097 (2007).
10. S.Capozziello, C.Corda, M. De Laurentis, *Phys. Lett. B* **699**, 255-259 (2008).
11. S. Bellucci, S. Capozziello, M. De Laurentis, V. Faraoni, *Phys. Rev. D* **79**, 104004 (2009).

# Elsevier instructions for the preparation of a 2-column format camera-ready paper in L<sup>A</sup>T<sub>E</sub>X

P. de Groot<sup>a\*</sup>, R. de Maas<sup>a†</sup>, X.-Y. Wang<sup>b</sup> and A. Sheffield<sup>a‡</sup>

<sup>a</sup>Mathematics and Computer Science Section, Elsevier Science B.V.,  
P.O. Box 103, 1000 AC Amsterdam, The Netherlands

<sup>b</sup>Economics Department, University of Winchester,  
2 Finch Road, Winchester, Hampshire P3L T19, United Kingdom

These pages provide you with an example of the layout and style for 100% reproduction which we wish you to adopt during the preparation of your paper. This is the output from the L<sup>A</sup>T<sub>E</sub>X document class you requested.

## 1. FORMAT

Text should be produced within the dimensions shown on these pages: each column 7.5 cm wide with 1 cm middle margin, total width of 16 cm and a maximum length of 19.5 cm on first pages and 21 cm on second and following pages. The L<sup>A</sup>T<sub>E</sub>X document class uses the maximum stipulated length apart from the following two exceptions (i) L<sup>A</sup>T<sub>E</sub>X does not begin a new section directly at the bottom of a page, but transfers the heading to the top of the next page; (ii) L<sup>A</sup>T<sub>E</sub>X never (well, hardly ever) exceeds the length of the text area in order to complete a section of text or a paragraph. Here are some references: [1,2].

### 1.1. Spacing

We normally recommend the use of 1.0 (single) line spacing. However, when typing complicated mathematical text L<sup>A</sup>T<sub>E</sub>X automatically increases the space between text lines in order to prevent sub- and superscript fonts overlapping

---

\*Footnotes should appear on the first page only to indicate your present address (if different from your normal address), research grant, sponsoring agency, etc. These are obtained with the `\thanks` command.

†For following authors with the same address use the `\addressmark` command.

‡To reuse an addressmark later on, label the address with an optional argument to the `\address` command, e.g. `\address[MCS D]`, and repeat the label as the optional argument to the `\addressmark` command, e.g. `\addressmark[MCS D]`.

one another and making your printed matter illegible.

### 1.2. Fonts

These instructions have been produced using a 10 point Computer Modern Roman. Other recommended fonts are 10 point Times Roman, New Century Schoolbook, Bookman Light and Palatino.

## 2. PRINTOUT

The most suitable printer is a laser or an inkjet printer. A dot matrix printer should only be used if it possesses an 18 or 24 pin printhead (“letter-quality”).

The printout submitted should be an original; a photocopy is not acceptable. Please make use of good quality plain white A4 (or US Letter) paper size. *The dimensions shown here should be strictly adhered to: do not make changes to these dimensions, which are determined by the document class.* The document class leaves at least 3 cm at the top of the page before the head, which contains the page number.

Printers sometimes produce text which contains light and dark streaks, or has considerable lighting variation either between left-hand and right-hand margins or between text heads and bottoms. To achieve optimal reproduction quality, the contrast of text lettering must be uniform,

sharp and dark over the whole page and throughout the article.

If corrections are made to the text, print completely new replacement pages. The contrast on these pages should be consistent with the rest of the paper as should text dimensions and font sizes.

### 3. TABLES AND ILLUSTRATIONS

Tables should be made with  $\LaTeX$ ; illustrations should be originals or sharp prints. They should be arranged throughout the text and preferably be included *on the same page as they are first discussed*. They should have a self-contained caption and be positioned in flush-left alignment with the text margin within the column. If they do not fit into one column they may be placed across both columns (using `\begin{table*}` or `\begin{figure*}`) so that they appear at the top of a page).

#### 3.1. Tables

Tables should be presented in the form shown in Table 1. Their layout should be consistent throughout.

Horizontal lines should be placed above and below table headings, above the subheadings and at the end of the table above any notes. Vertical lines should be avoided.

If a table is too long to fit onto one page, the table number and headings should be repeated above the continuation of the table. For this you have to reset the table counter with `\addtocounter{table}{-1}`. Alternatively, the table can be turned by  $90^\circ$  ('landscape mode') and spread over two consecutive pages (first an even-numbered, then an odd-numbered one) created by means of `\begin{table}[h]` without a caption. To do this, you prepare the table as a separate  $\LaTeX$  document and attach the tables to the empty pages with a few spots of suitable glue.

#### 3.2. Useful table packages

Modern  $\LaTeX$  comes with several packages for tables that provide additional functionality. Below we mention a few. See the documentation of the individual packages for more details. The

Table 2: The next-to-leading order (NLO) results *without* the pion field.

$\Lambda$ (MeV)	140	150	175	200	225	250	Exp.	$v_{18}$ [?]
$r_d$ (fm)	1.973	1.972	1.974	1.978	1.983	1.987	1.966(7)	1.967
$Q_d$ (fm <sup>2</sup> )	0.259	0.268	0.287	0.302	0.312	0.319	0.286	0.270
$P_D$ (%)	2.32	2.83	4.34	6.14	8.09	9.90	—	5.76
$\mu_d$	0.867	0.864	0.855	0.845	0.834	0.823	0.8574	0.847
$\mathcal{M}_{M1}$ (fm)	3.995	3.989	3.973	3.955	3.936	3.918	—	3.979
$\mathcal{M}_{GT}$ (fm)	4.887	4.881	4.864	4.846	4.827	4.810	—	4.859
$\delta_{1B}^{VP}$ (%)	-0.45	-0.45	-0.45	-0.45	-0.45	-0.44	—	-0.45
$\delta_{1B}^{C2:C}$ (%)	0.03	0.03	0.03	0.03	0.03	0.03	—	0.03
$\delta_{1B}^{C2:N}$ (%)	-0.19	-0.19	-0.18	-0.15	-0.12	-0.10	—	-0.21

The experimental values are given in ref. [4].



Table 1  
The next-to-leading order (NLO) results *without* the pion field.

$\Lambda$ (MeV)	140	150	175	200
$r_d$ (fm)	1.973	1.972	1.974	1.978
$Q_d$ (fm <sup>2</sup> )	0.259	0.268	0.287	0.302
$P_D$ (%)	2.32	2.83	4.34	6.14
$\mu_d$	0.867	0.864	0.855	0.845
$\mathcal{M}_{M1}$ (fm)	3.995	3.989	3.973	3.955
$\mathcal{M}_{GT}$ (fm)	4.887	4.881	4.864	4.846
$\delta_{1B}^{VP}$ (%)	-0.45	-0.45	-0.45	-0.45
$\delta_{1B}^{C^2:C}$ (%)	0.03	0.03	0.03	0.03
$\delta_{1B}^{C^2:N}$ (%)	-0.19	-0.19	-0.18	-0.15

The experimental values are given in ref. [4].

packages can be found in L<sup>A</sup>T<sub>E</sub>X's `tools` directory.

`array` Various extensions to L<sup>A</sup>T<sub>E</sub>X's `array` and `tabular` environments.

`longtable` Automatically break tables over several pages. Put the table in the `longtable` environment instead of the `table` environment.

`dcolumn` Define your own type of column. Among others, this is one way to obtain alignment on the decimal point.

`tabularx` Smart column width calculation within a specified table width.

`rotating` Print a page with a wide table or figure in landscape orientation using the `sidewaystable` or `sidewaysfigure` environments, and many other rotating tricks. Use the package with the `figuresright` option to make all tables and figures rotate in clockwise. Use the starred form of the `sideways` environments to obtain full-width tables or figures in a two-column article.

### 3.3. Line drawings

Line drawings may consist of laser-printed graphics or professionally drawn figures attached to the manuscript page. All figures should be clearly displayed by leaving at least one line of spacing above and below them. When placing a

figure at the top of a page, the top of the figure should align with the bottom of the first text line of the other column.

Do not use too light or too dark shading in your figures; too dark a shading may become too dense while a very light shading made of tiny points may fade away during reproduction.

All notations and lettering should be no less than 2 mm high. The use of heavy black, bold lettering should be avoided as this will look unpleasantly dark when printed.

### 3.4. PostScript figures

Instead of providing separate drawings or prints of the figures you may also use PostScript files which are included into your L<sup>A</sup>T<sub>E</sub>X file and printed together with the text. Use one of the packages from L<sup>A</sup>T<sub>E</sub>X's `graphics` directory: `graphics`, `graphicx` or `epsfig`, with the `\usepackage` command, and then use the appropriate commands (`\includegraphics` or `\epsfig`) to include your PostScript file.

The simplest command is:  
`\includegraphics{file}`, which inserts the PostScript file `file` at its own size. The starred version of this command:  
`\includegraphics*{file}`, does the same, but clips the figure to its bounding box.

With the `graphicx` package one may specify a series of options as a key-value list, e.g.:

```
\includegraphics[width=15pc]{file}
\includegraphics[height=5pc]{file}
\includegraphics[scale=0.6]{file}
\includegraphics[angle=90,width=20pc]{file}
```

See the file `grfguide`, section “Including Graphics Files”, of the `graphics` distribution for all options and a detailed description.

The `epsfig` package mimicks the commands familiar from the package with the same name in  $\text{\LaTeX}2.09$ . A PostScript file `file` is included with the command `\psfig{file=file}`.

Grey-scale and colour photographs cannot be included in this way, since reproduction from the printed CRC article would give insufficient typographical quality. See the following subsections.



Figure 1. Good sharp prints should be used and not (distorted) photocopies.

### 3.5. Black and white photographs

Photographs must always be sharp originals (*not screened versions*) and rich in contrast. They will undergo the same reduction as the text and should be pasted on your page in the same way as line drawings.

### 3.6. Colour photographs

Sharp originals (*not transparencies or slides*) should be submitted close to the size expected in publication. Charges for the processing and printing of colour will be passed on to the

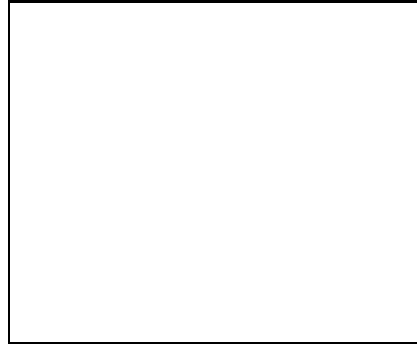


Figure 2. Remember to keep details clear and large enough.

author(s) of the paper. As costs involved are per page, care should be taken in the selection of size and shape so that two or more illustrations may be fitted together on one page. Please contact the Author Support Department at Elsevier (E-mail: [authorsupport@elsevier.nl](mailto:authorsupport@elsevier.nl)) for a price quotation and layout instructions before producing your paper in its final form.

## 4. EQUATIONS

Equations should be flush-left with the text margin;  $\text{\LaTeX}$  ensures that the equation is preceded and followed by one line of white space.  $\text{\LaTeX}$  provides the document class option `fleqn` to get the flush-left effect.

$$H_{\alpha\beta}(\omega) = E_{\alpha}^{(0)}(\omega)\delta_{\alpha\beta} + \langle \alpha | W_{\pi} | \beta \rangle \quad (1)$$

You need not put in equation numbers, since this is taken care of automatically. The equation numbers are always consecutive and are printed in parentheses flush with the right-hand margin of the text and level with the last line of the equation. For multi-line equations, use the `eqnarray` environment.

For complex mathematics, use the `\mathcal{M}Smath` package. This package sets the math indentation to a positive value. To keep the equations flush left, either load the `espcrc` package *after* the `\mathcal{M}Smath` package or set the command

`\mathindent=0pt` in the preamble of your article.

## REFERENCES

1. S. Scholes, Discuss. Faraday Soc. No. 50 (1970) 222.
2. O.V. Mazurin and E.A. Porai-Koshits (eds.), Phase Separation in Glass, North-Holland, Amsterdam, 1984.
3. Y. Dimitriev and E. Kashchieva, J. Mater. Sci. 10 (1975) 1419.
4. D.L. Eaton, Porous Glass Support Material, US Patent No. 3 904 422 (1975).

References should be collected at the end of your paper. Do not begin them on a new page unless this is absolutely necessary. They should be prepared according to the sequential numeric system making sure that all material mentioned is generally available to the reader. Use `\cite` to refer to the entries in the bibliography so that your accumulated list corresponds to the citations made in the text body.

Above we have listed some references according to the sequential numeric system [1,2,3,4].